

# Measurement of High- $Q^2$ Charged and Neutral Current Deep Inelastic $e^+p$ Scattering Cross Sections with a Longitudinally Polarised Positron Beam at HERA

---

**Trevor Stewart\***

*On behalf of the ZEUS Collaboration - University of Toronto*

*E-mail: [stewartt@physics.utoronto.ca](mailto:stewartt@physics.utoronto.ca)*

Measurements of the cross sections for neutral current (NC) and charged current (CC) deep inelastic scattering in  $e^+p$  collisions with a longitudinally polarised positron beam are presented. The measurements are based on a data sample with an integrated luminosity of  $135.48 \text{ pb}^{-1}$  for NC and  $132 \text{ pb}^{-1}$  for CC collected with the ZEUS detector at HERA in 2006 and 2007 at a centre-of-mass energy of 318 GeV. The total CC cross section are presented at positive and negative values of the longitudinal polarization of the positron beams and are used to determine a lower limit on the mass of a hypothetical right-handed W boson. The single differential NC (CC) cross sections  $d\sigma/dQ^2$ ,  $d\sigma/dx$  and  $d\sigma/dy$  are presented for  $Q^2 > 185 \text{ GeV}^2$  ( $Q^2 > 200 \text{ GeV}^2$ ). The reduced NC (CC) cross sections  $\tilde{\sigma}$  are presented. The structure function  $x\tilde{F}_3$  is determined by combining the  $e^+p$  NC reduced cross sections with the previously measured  $e^-p$  [2] measurements. Reduced cross sections from a high- $Q^2$  NC  $e^+p$  analysis at high- $x$  are presented.

The measurements from the CC, NC and high- $x$  NC analyses agree well with the predictions of the Standard Model (SM).

*The 2011 Europhysics Conference on High Energy Physics, EPS-HEP 2011,  
July 21-27, 2011  
Grenoble, Rhône-Alpes, France*

---

\*Speaker.

## 1. Introduction

Deep inelastic scattering (DIS) of leptons off nucleons has proved to be a key tool for understanding the structure of the proton. The neutral current (NC) process at HERA,  $e^-(e^+)p \rightarrow e^-(e^+)X$ , is mediated by the exchange of a  $\gamma$  or  $Z^0$  boson, while the charged current (CC) process,  $e^-(e^+)p \rightarrow \nu(\bar{\nu})X$ , is mediated by the exchange of a  $W^\pm$  boson.

The NC and CC processes are described by three invariant variables:  $Q^2$ , the negative four momentum transfer squared;  $x$ , the Bjorken scaling variable;  $y$ , the inelasticity. These variables are related by  $Q^2 = sxy$ , where  $s$  is the centre-of-mass energy squared, neglecting the mass of the proton and electron.

In 2002, HERA was upgraded to provide longitudinally polarised  $e^\pm$  beams. The polarisation of the  $e^\pm$  beam is defined as  $P_e = (N_R - N_L)/(N_R + N_L)$ , where  $N_R$  ( $N_L$ ) is the number of right (left) handed  $e^\pm$  in the beam.

The NC and CC[1] cross section measurements were made using  $e^+p$  data collected in 2006-2007, with a proton beam energy of  $E_p = 920$  GeV, and a  $e^+$  beam of  $E_e = 27.5$  GeV ( $\sqrt{s} = 318$  GeV). The NC (CC)  $e^+p$  data set was divided into a  $\mathcal{L} = 78.8$  pb $^{-1}$  ( $\mathcal{L} = 75.8$  pb $^{-1}$ )  $P_e = +32\%$  ( $P_e = +33\%$ ) sample and a  $\mathcal{L} = 56.7$  pb $^{-1}$  ( $\mathcal{L} = 56.0$  pb $^{-1}$ )  $P_e = -36\%$  ( $P_e = -36\%$ ) sample, where  $\mathcal{L}$  and  $P_e$  are the luminosity and polarisation respectively. The values of  $\mathcal{L}$  and  $P_e$  are not identical for NC and CC analyses due to differences between the NC and CC data selection.

## 2. Cross sections

The polarised CC reduced cross-section can be written as follows:

$$\begin{aligned} \tilde{\sigma}_{CC}^{e^{-\{+\}}p} &= (1 \pm P_e) \tilde{\sigma}_{CC, P_e=0}^{e^{-\{+\}}p} = \\ & (1 \pm P_e) x [u\{\bar{u}\} + c\{\bar{c}\}] + (1-y)^2 (\bar{d}\{d\} + \bar{s}\{s\}) \end{aligned} \quad (2.1)$$

where, for example, the parton distribution function (PDF)  $\bar{u}(x, Q^2)$  gives the number density of anti-up quarks for a given  $x$  and  $Q^2$ . Measurement of the  $e^+p$  ( $e^-p$ ) cross-section is directly sensitive to the d-quark (u-quark) density of the proton. Additionally, the CC cross-section scales linearly with  $e^\pm$  beam polarisation.

The NC born-level cross section is given by

$$\frac{d^2 \sigma_{NC}^{e^\pm p}}{dx dQ^2} = \frac{2\pi\alpha^2}{xQ^4} [Y_+ \tilde{F}_2 \mp Y_- x\tilde{F}_3 - y^2 \tilde{F}_L] \quad (2.2)$$

$$\tilde{\sigma}_{NC}^{e^\pm p} = \frac{xQ^4}{2\pi\alpha^2} \frac{1}{Y_+} \frac{d^2 \sigma_{NC}^{e^\pm p}}{dx dQ^2} = \tilde{F}_2 \mp \frac{Y_-}{Y_+} x\tilde{F}_3 - \frac{y^2}{Y_+} \tilde{F}_L \quad (2.3)$$

$$\tilde{F}_2 = F_2^\gamma + \kappa(-v_e \pm P_e a_e) F_2^{\gamma Z} + \kappa^2 (v_e^2 + a_e^2 \pm 2P_e v_e a_e) F_2^Z \quad (2.4)$$

$$x\tilde{F}_3 = \kappa(-a_e \mp P_e v_e) x F_3^{\gamma Z} + \kappa^2 (2v_e a_e \pm P_e (v_e^2 + a_e^2)) x F_3^Z \quad (2.5)$$

where  $\tilde{\sigma}_{NC}^{e^\pm p}$  is the reduced cross-section,  $Y_\pm = 1 \pm (1-y)^2$ , and  $\kappa = \frac{1}{\sin^2 2\theta_w} \frac{Q^2}{Q^2 + M_Z^2}$ .  $\tilde{F}_2$ ,  $x\tilde{F}_3$  and  $\tilde{F}_L$  are the generalised structure functions, and can be written as a linear combinations of the hadronic

structure functions,  $F_2$ ,  $F_2^{\gamma Z^0}$  and  $F_2^{Z^0}$ , due to  $\gamma$  exchange,  $\gamma - Z^0$  interference, and  $Z^0$  exchange respectively. The  $x\tilde{F}_3$  structure function becomes significant at high- $Q^2$  reducing the  $e^+p$  cross-section.  $\tilde{F}_L$  is expected to contribute only at large  $y$ , and be negligible at high- $Q^2$  and high- $x$ . Unlike the CC case the dependence of the NC cross-sections on lepton beam polarisation is not linear.

### 3. Results

#### 3.1 Unpolarised CC and NC DIS

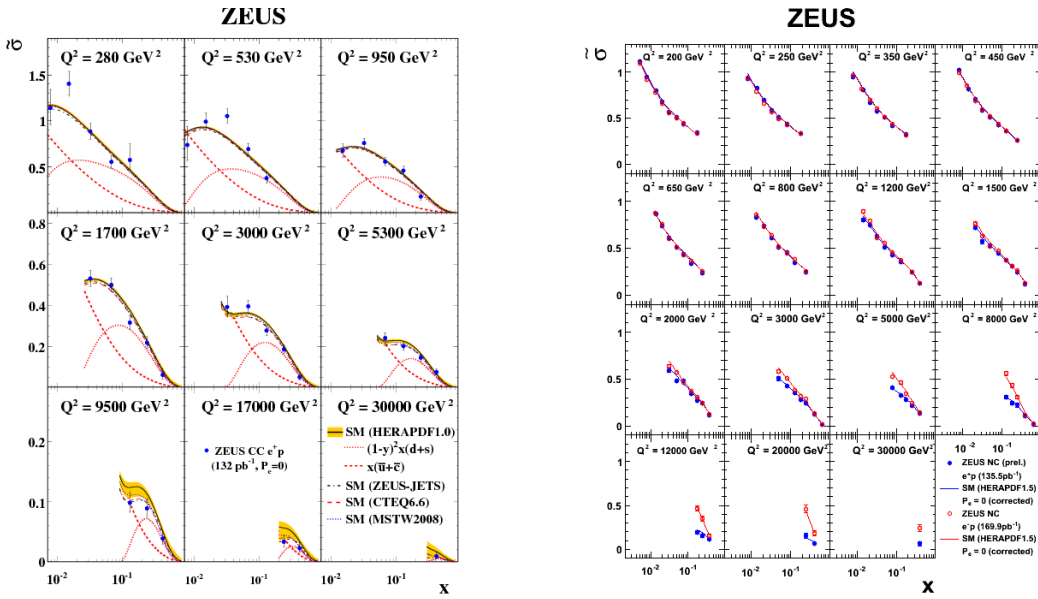


**Figure 1:** The  $e^+p$  CC DIS (left) and  $e^\pm p$  NC DIS (right) reduced cross-section in as a function of  $x$  at fixed  $Q^2$ . The circles represent the data points and the curves are SM predictions using different PDFs. The dashed and dotted lines on the left plot show the contributions of  $(d+s)$  and  $x(\bar{u}+\bar{c})$ , respectively.

The CC and NC polarised data can be combined into an effectively unpolarised,  $P_e = 0$ , data set after correcting for any residual polarisations. The  $e^+p$  CC DIS and  $e^\pm p$  NC DIS reduced cross-sections ( $e^-p$  NC cross-section published in [2]) as a function of  $x$  in fixed  $Q^2$  bins are shown in Fig. 1. The SM predictions evaluated using different PDFs give a good description of the data. The contributions of the PDF combinations  $(d+s)$  and  $x(\bar{u}+\bar{c})$  to the  $e^+p$  CC DIS reduced cross-section are presented in Fig. 1 (left).

The significant difference between the NC  $e^+p$  and  $e^-p$  cross-sections is observed at high- $Q^2$  due to the  $x\tilde{F}_3$  contribution, which suppresses the  $e^+p$  cross-section with respect to the  $e^-p$  data. The SM predictions are in good agreement with the reduced cross section measurement.

The structure function  $x\tilde{F}_3$  is measured from the difference of the reduced cross sections:

$$\tilde{\sigma}^{e^-p} - \tilde{\sigma}^{e^+p} = \frac{Y_-}{Y_+} 2x\tilde{F}_3 \quad (3.1)$$

As  $x\tilde{F}_3$  is expected to contribute at high- $Q^2$ , only measurements with  $Q^2 > 1500 \text{ GeV}^2$  are included in the result. The  $x\tilde{F}_3$  results are shown in Fig. 2. At  $Q^2 = 1500 \text{ GeV}^2$  the contribution of  $x\tilde{F}_3$  is still

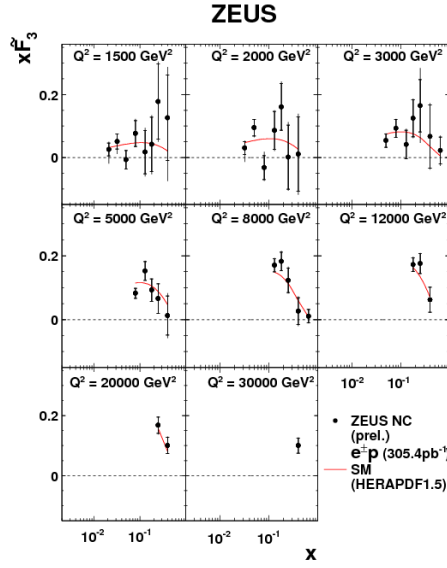


**Figure 2:** The circles represent the  $x\tilde{F}_3$  data points in bins of  $Q^2$  and as a function of  $x$  and the curves show the predictions of the SM evaluated using HERAPDF1.5.

small, but increases with larger  $Q^2$  values as expected. The SM prediction is in excellent agreement with the measured  $x\tilde{F}_3$  values. The  $e^-$  and  $e^+$  data sets are the largest collected at ZEUS; therefore it is the most precise  $x\tilde{F}_3$  measurement with ZEUS.

### 3.2 Polarised CC and NC DIS

The total  $e^+p$  CC DIS cross-section, corrected to the Born level in the electroweak (EW) interaction, in the kinematic region  $Q^2 > 200 \text{ GeV}^2$  was measured to be:

$$\sigma^{CC}(P_e = -0.36 \pm 0.014) = 22.9 \pm 0.82 \text{ (stat.)} \pm 0.60 \text{ (lumi.)} \pm 0.40 \text{ (syst.) pb} \quad (3.2)$$

$$\sigma^{CC}(P_e = +0.33 \pm 0.012) = 48.0 \pm 1.01 \text{ (stat.)} \pm 1.25 \text{ (lumi.)} \pm 0.77 \text{ (syst.) pb} \quad (3.3)$$

In Fig. 3 (right) the total  $e^+p$  CC cross-section is shown for both positive and negative values of the  $e^+$  beam polarisation along with previous ZEUS and H1  $e^+p$  and  $e^-p$  data[3, 4, 5, 6, 7, 8]. The SM predictions, which predict an increase (decrease) in  $\tilde{\sigma}$  for positive (negative)  $e^+$  polarisation, are in good agreement with the data. By extrapolating the total cross-section to  $P_e = -1$  an upper limit on the cross-section can be converted to a lower limit on the mass of the right-handed W boson,  $W_R$ . The limits obtained are:

$$\sigma^{CC}(P_e = -1) < 2.9 \text{ pb at 95\% CL} \quad (3.4)$$

$$M_{W_R} > 198 \text{ GeV at 95\% CL} \quad (3.5)$$

The results are consistent with zero as the SM predicts.

The single differential  $e^+p$  CC cross-sections  $d\sigma/dQ^2$ ,  $d\sigma/dx$  and  $d\sigma/dy$  were measured for both positive and negative  $e^+$  beam polarisation values. The cross-sections exhibit an overall difference between the negative and positive polarisations and are consistent with the SM.

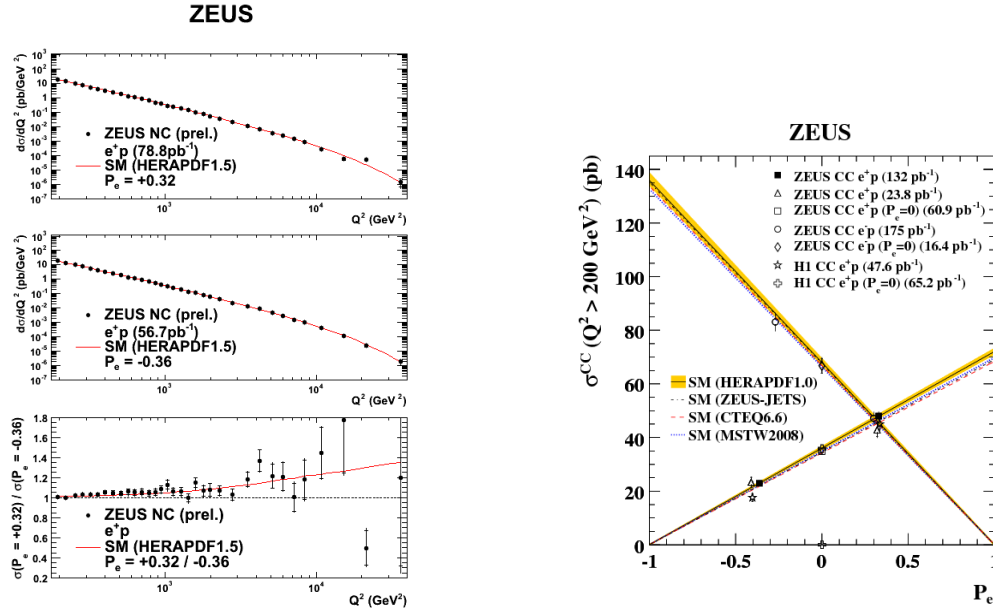


**Figure 3:** (left) Single differential NC  $e^+p$  cross sections  $d\sigma/dQ^2$  for positive (top) and negative (middle)  $e^+$  beam polarisation and the ratio of  $d\sigma/dQ^2$  using negative and positive polarisation (bottom). The circles represent the data points and the curves show the predictions of the SM evaluated using HERAPDF1.5. (right) Total  $e^\pm p$  CC cross sections as a function of the lepton beam polarisation,  $P_e$ .

The single differential NC  $e^+p$  cross-section,  $d\sigma/dQ^2$ , is shown in Fig. 3 (left) for both positive and negative  $e^+$  beam polarisation values. The cross-sections,  $d\sigma/dx$  and  $d\sigma/dy$  for both  $Q^2 > 185 \text{ GeV}^2$  and  $Q^2 > 3000 \text{ GeV}^2$  were extracted for each lepton beam polarisation as well. All single differential cross-sections are well described by SM predictions. The reduced cross-sections for both positive and negative  $e^+$  beam polarisations were measured and agree well with the SM predictions. Parity violation is clearly seen in  $d\sigma/dQ^2$  and the reduced cross-section.

#### 4. High- $Q^2$ NC $e^+p$ Cross-sections at high- $x$

At high- $x$  the PDFs are poorly constrained and the differences between different PDF sets increase greatly. This is chiefly due to the limited information at high- $x$  on the structure functions in DIS. The high- $Q^2$  analysis described previously in this text only measures the reduced cross-section up to  $x = 0.65$ . There are multiple reasons for this: the small cross-section at high- $x$ , limitations in the beam energy, and the analysis techniques. With the beginning of data taking at the Large Hadron Collider (LHC) this high- $x$  regime is increasingly relevant eg. for the highest mass searches.

##### 4.1 Reconstruction technique

The typical event topology of a NC event in the ZEUS detector is as follows: a scattered electron and a jet from the struck quark clearly identified in the detector which balances the electron in  $\phi$ . The proton remnant, the remains of the proton after being struck by the electron, is mainly lost down the beampipe. To reconstruct the kinematics of a NC event the double-angle method, using

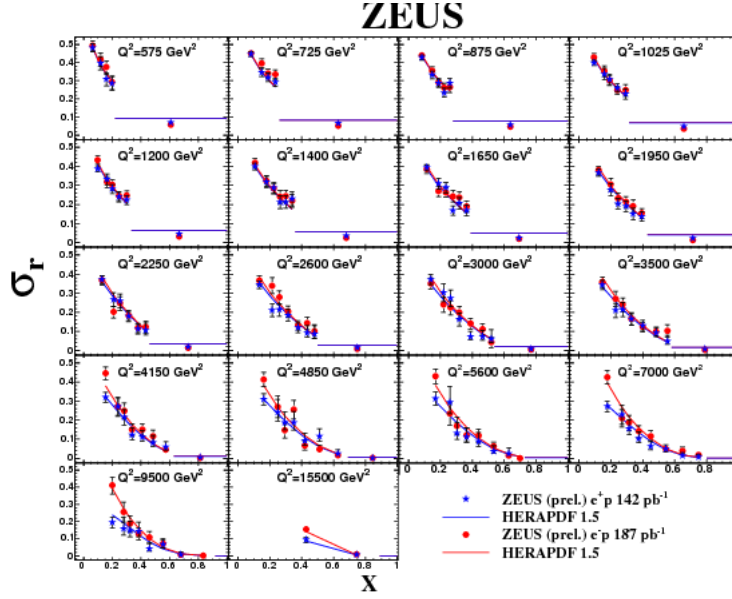


**Figure 4:** The high- $x$  reduced cross sections for  $e^+$  (blue) and  $e^-$  (red) in bins of  $Q^2$  and as a function of  $x$ . The highest  $x$  point for each  $Q^2$  bin corresponds to the integrated cross section bin. The points are data and the lines the HERAPDF1.5 predictions.

the angles of the scattered electron and struck quark. However, this limits the maximum value of  $x$  that can be measured. As  $x$  increases the jet becomes increasingly forward, until it can no longer be used to reconstruct the kinematic variables (with most of the jet being lost down the beampipe). At the point where the jet is not well reconstructed we define a  $x$  value,  $x_{limit}$ , that depends on  $Q^2$ . The technique developed for this analysis uses the hadronic system to measure  $x$  by the angle of the jet produced by the scattered quark for  $x < x_{limit}$ . Where the jet is not well reconstructed  $x$  cannot be reconstructed but is within the range  $x_{limit} < x < 1$ . For values of  $x_{limit} < x < 1$  an integrated cross section is calculated. An analysis using a similar method to that shown here was published for HERA-I [9]. The jet definition used in this analysis is as follows:  $E_{t,jet} > 10\text{GeV}$  and  $\theta_{jet} > 0.11$ .

Fig. 4 shows the reduced cross sections for both  $x$  regions:  $x < x_{limit}$  and the integrated bin  $x_{limit} < x < 1$ . In addition to the  $e^+$  results,  $e^-$  results from HERA-II that were made preliminary for DIS2010 are shown. The SM predictions for both  $e^+$  and  $e^-$  are in good agreement with the data. As in the case of the standard NC analysis, the difference of the cross sections at high- $Q^2$  is due to  $x\tilde{F}_3$  and hence it is possible to extract a high- $x$   $x\tilde{F}_3$  structure function.

## 5. Summary

Polarised and unpolarised  $e^+p$  high- $Q^2$  NC and CC DIS cross-sections have been presented. The total  $e^+p$  CC cross-section at both positive and negative polarisation was shown, and is consistent with 0 when extrapolated to  $P_e = -1$ . The NC cross-section  $d\sigma/dQ^2$  and polarised reduced cross-sections, clearly show parity violation at high- $Q^2$ . The unpolarised  $e^+p$  NC reduced cross-section was presented with the previously measured  $e^-p$  cross-section showing the effect of  $x\tilde{F}_3$  at

high- $Q^2$ . The structure function  $x\tilde{F}_3$  has been extracted. Both the polarised cross sections and the  $x\tilde{F}_3$  structure function provide a test of EW theory. The SM predictions are in good agreement with the results of both the CC and NC analyses. The newly measured NC reduced cross-sections can be used to better constrain the proton PDFs.

In addition to the standard NC analysis results, high- $x$  NC reduced cross section have been shown. The SM predictions are in good agreement with the results and these data will help constrain the PDFs at high- $x$ , a hitherto poorly studied region.

## References

- [1] ZEUS Collab., H. Abramowicz et al., *Eur. Phys. J C* 70, 945 (2010).
- [2] ZEUS Collab., S. Chekanov et al., *Eur. Phys. J C* 62, 625 (2008).
- [3] ZEUS Collab., S. Chekanov et al., *Phys. Lett B* 539, 197 (2002). Erratum in *Phys. Lett. B* 552, 308 (2003).
- [4] ZEUS Collab., S. Chekanov et al., *Eur. Phys. J C* 32, 1 (2003).
- [5] ZEUS Collab., S. Chekanov et al., *Phys. Lett B* 637, 28 (2006).
- [6] ZEUS Collab., S. Chekanov et al., *Eur. Phys. J C* 61, 223 (2009).
- [7] H1 Collab., C. Adloff et al., *Eur.Phys.J C* 30, 1 (2003).
- [8] H1 Collab., A. Aktas et al., *Phys. Lett B* 634, 173 (2006).
- [9] ZEUS Collab., S. Chekanov et al., *Eur. Phys. J C* 49 523 (2007).